Water Science & Technology

Water Science & Technology Vol 00 No 0, 1 doi: 10.2166/wst.2021.215

Nitrate reduction by electrochemical processes using copper electrode: evaluating operational parameters aiming low nitrite formation

T. F. Beltrame[a,*], F. M. Zoppas[b], J. Z. Ferreira[a], F. A. Marchesini[b] and A. M. Bernardes[a]
[a] Laboratório de Corrosão, Proteção e Reciclagem de Materiais LACOR-UFRGS (Universidade Federal do Rio Grande do Sul), Av. Bento Gonçalves, 9500, Porto Alegre, RS, Brazil
[b] Instituto de Investigaciones en Catálisis y Petroquímica (INCAPE-CONICET), Santiago del Estero 2829, CP 3000, Santa Fe, Argentina
*Corresponding author. E-mail: thiagofbeq@gmail.com

FMZ, 0000-0002-7747-2183

ABSTRACT

This work aims to present different electroreduction and electrocatalytic processes configurations to treat nitrate contaminated water. The parameters tested were: current density, cell potential, electrode potential, pH values, cell type and catalyst use. It was found that the nitrite ion is present in all process variations used, being the resulting nitrite concentration higher in an alkaline pH. The increase in current density on galvanostatic operation mode provides a greater reduction of nitrate (64%, 1.4 mA cm^{-2}) if compared to the potentiostatic (20%) and constant cell potential (37%) configurations. In a dual-chamber cell the nitrate reduction with current density of 1.4 mA cm^{-2} was tested and obtained as a NO_3^- reduction of 85%. The use of single chamber cell presented 32 $\pm$ 3% of nitrate reduction, indicating that in this cell type the nitrate reduction is smaller than in dual-chamber cell (64%). The presence of a Pd catalyst with 3.1% wt. decreased the nitrite (1.0 N-mg L^{-1}) and increased the gaseous compounds (9.4 N-mg L^{-1}) formation. The best configuration showed that, by fixing the current density, the highest nitrate reduction is obtained and the pH presents a significant influence during the tests. The use of the catalyst decreased the nitrite and enhanced the gaseous compounds formation.

Key words: copper electrode, electrocatalysis, electroreduction, nitrate reduction, operational parameters, Pd catalyst

HIGHLIGHTS

- Electroreduction can be used to treat contaminated water with a high nitrate concentration.
- Galvanostatic mode promotes a high nitrate reduction.
- Increase in current density improves the nitrate reduction.
- The Pd catalyst decreases the nitrite and increases the formation of the gaseous compounds.
- This system does not need a catalyst separation stage of water after reaction.

INTRODUCTION

Nitrate ($NO_{3(aq)}^-$) is an ion present in surface and groundwater and its presence in these systems can cause damage to the environment (Smith & Schindler 2009; Wang *et al.* 2021) and to human health (Cameron *et al.* 2013; Wang *et al.* 2021). Among different methods used for the treatment of water contaminated with nitrate, the membrane separation processes (MSP) stand out. However, MSPs generate a concentrated solution (Sahli *et al.* 2008), transferring the problem to a residue that needs to be properly treated or stored.

Other options for the treatment of water contaminated with nitrates are the electroreduction and the catalytic processes, in which the nitrate ion ($NO_{3(aq)}^-$) can be reduced to nitrogen gas ($N_{2(g)}$). To use the electroreduction process on an industrial scale it is necessary to study the different operational parameters that can influence the system, as each operational characteristic may have an effect on the ion removal efficiency and on the different products that can be formed, such as ammonium ($NH_{4(aq)}^+$), nitrite ($NO_{2(aq)}^-$) and gaseous compounds (ideally nitrogen gas) (Beltrame *et al.* 2018). Among different parameters, pH, current density, cell (Beltrame *et al.* 2018) and electrode potential can affect nitrate ion reduction and, consequently, the products formation (Reyter *et al.* 2008; Su *et al.* 2016; Xu *et al.* 2018). Conversely, in the catalytic processes, the parameters that influence the reduction efficiency are: the type of catalyst support, reducing agent, pH, composition of the catalyst active phase, type of reactor, among others (Martínez *et al.* 2017).

To improve conversion or selectivity, a combined process, electrocatalysis, may be used, to increase the efficiency of the global process, when compared to using them separately (electroreduction or catalysis). For electroreduction and electrocatalytic processes, the electrode material is also an important parameter. Several electrodes can be used to propitiate the nitrate reduction, such as nickel (Simpson & Johnson 2004; Gwak *et al.* 2019) and iron (Jonoush *et al.* 2020). However, copper (Pérez-Gallent *et al.* 2017; Beltrame *et al.* 2019) is the one the most used, due to the similarity of the energy levels of the copper 'd'-orbital with the nitrate Lumo π* molecular orbital (Garcia-Segura *et al.* 2018).

In the electrochemical reduction of nitrate, the electrokinetics is generally slow, due to the high energy of the lowest unoccupied π molecular orbital of nitrate, which makes the injection of charge into this orbital unfavorable. However, due to the similarity in energy levels of the 'd' orbitals of some metals, such as copper, and the unoccupied π molecular orbital of nitrate, these metals present the ability to promote the electrochemical reduction of $NO_{3(aq)}^{-}$' (Garcia-Segura *et al.* 2018), transferring electrons more easily to the adsorbed nitrate, and favoring the nitrate electroreduction (Khomutov & Stamkulov 1971; Huang *et al.* 1990). Thus, it was chosen to use the copper electrode due to its low cost, high stability, catalytic activity (Zhang *et al.* 2019) and high corrosion resistance. Dortsiou *et al.* (2013) used, for instance, a Sn like electrode and, even with good selectivity for nitrogen, an electrode corrosion was observed (Dortsiou *et al.* 2013).

For the electrocatalytic reduction of nitrate, there are studies that focus on the modification of the surface of the electrodes with the use of nanoparticles of a noble metal, for instance, palladium (Pd) (Estudillo-Wong *et al.* 2011; Zhang *et al.* 2014) and also non-noble metals (Ye *et al.* 2020). A distinct approach is the addition of the catalyst not in the electrode surface, but in the cathode compartment of the reactor (Beltrame *et al.* 2019, 2020).

In electroreduction, the energy that is given to the system promotes water hydrolysis, forming hydrogen gas ($H_{2(g)}$) and oxygen gas ($O_{2(g)}$). The hydrogen formed acts as a reducing agent on the copper surface, promoting the reduction of nitrate to nitrite and reducing nitrite to ammonium or gaseous compounds (Bosko *et al.* 2014):

$$2NO_{3(aq)}^{-} + 5H_{2(g)} \rightarrow N_{2(g)} + 2OH_{(aq)}^{-} + 4H_2O_{(l)} \quad (1)$$

$$2NO_{3(aq)}^{-} + 8H_{2(g)} \rightarrow 2NH_{4(aq)}^{+} + 4OH_{(aq)}^{-} + 2H_2O_{(l)} \quad (2)$$

Reactions 1 and 2 demonstrate that the nitrate ion reduction generates hydroxyl, promoting an increase in the pH value, what increases the selectivity of the reaction towards the production of the ammonium ion, $NH_{4(aq)}^{+}$, instead of $N_{2(g)}$ (Tokazhanov *et al.* 2020). The desirable product of nitrate reduction in drinking water is nitrogen gas, although the byproducts ammonium or nitrite are obtained in electrochemical treatments (Garcia-Segura *et al.* 2018).

It is a challenge to find an ideal operational parameter to obtain nitrate electroreduction: in this sense, some parameters should be analyzed, such as current density, pH values, operation mode, cell potential, cell type and catalyst use. Therefore, in this paper, operational parameters for nitrate electroreduction process were studied, aiming at low nitrite ion formation, by using the copper electrode to increase the ammonium and gaseous compounds production. For this, the following parameters were studied: current density, pH, cell potential, electrode potential and cell type. Three operational modes were evaluated: galvanostatic, potentiostatic and constant cell potential. In the galvanostatic mode, different current densities were fixed, while in the potentiostatic mode the cathode potential was fixed (Garcia-Segura *et al.* 2018). In the constant cell potential operational mode, the cell potential was fixed along the experiments.

Finally, the influence of Pd catalyst on nitrate reduction was also tested. It is important to highlight that usually palladium catalyst supported on alumina is used in the powder form to reduce nitrate (Martínez *et al.* 2017; Tokazhanov *et al.* 2020), a subsequent unitary operation to separate the catalyst of the nitrate solution is necessary.

In this study, the catalyst was placed close to the copper electrode, and not added to the nitrate solution. Therefore, there was no need for a further filtration step to separate the catalyst from the solution, yielding a novel electrocatalytic system.

EXPERIMENTAL

Work solutions

Two different sodium nitrate solutions, with 600 mg L^{-1} (135.5 N-mg L^{-1}) or 100 mg L^{-1} (22.5 N-mg L^{-1}) ($NaNO_3 > 99\%$, Reagen, Brazil), were used to study the nitrate ion reduction. A sulphate solution of 1,400 mg L^{-1} (Labsynth, Brazil) was used to maintain the system conductivity when a dual chamber cell was

used. In some cases, when a single chamber cell was used, a sulphate solution (300 mg L^{-1}) was also added as electrolyte. Palladium chloride P.A. ($PdCl_2$ Neon, Brazil) was used in the pellet's catalyst synthesis. Alumina (Ketjen CK300) with 198 $m^2\ g^{-1}$ surface area and 0.5 mL g^{-1} pore volume was used as the support in the pellet's synthesis (1.2% wt. and 3.1% wt.). All solutions were prepared with distilled and deionized water. When the pH was adjusted, solutions of H_2SO_4 3 mol L^{-1} (Dinâmica, Brazil) or NaOH 3 mol L^{-1} (Dinâmica, Brazil) were used.

Experimental setup

A single chamber cell (SCC) and a dual-chamber cell (DCC) (Beltrame *et al.* 2018), separated by a cationic membrane (HDX 100, supplied by Hidrodex®) with 16 cm^2, were used in the experiments. For both cells, an electrode of $Ti70/TiO_230RuO_2$ (geometric area of 15 cm^2) and an electrode of copper (15 cm^2) were used as the anode and cathode, respectively. For the SCC, 170 mL of $NaNO_3$ solution was utilized. In the DCC, the sodium nitrate solution was placed in the cathodic compartment, whereas on the anodic side, sodium sulphate was used. The volume of the solution in each chamber was 170 mL.

The catalyst preparation was accomplished with the methodology used by Beltrame *et al.* (2020) and as briefly explained here: alumina pellets, $PdCl_2$ (0.056 M) and HCl (0.1 M) were added in a beaker with magnetic stirring and heated up to 80 °C, the temperature was maintained until all the solution was evaporated. Then, the pellets were calcined (500 °C for 4 hours) and activated with hydrazine (1 M) for 1 hour and at 40 °C. The catalyst was washed and dried for 12 hours at 80 °C. The palladium catalyst (0.25 g inside a 100% polyester fabric bag with geometric area of 30 cm^2) was placed in the cell near the copper electrode. This mode of configuration was chosen instead of carrying out an electrode synthesis, or using the catalyst as a power form, because it is a simple way of scaling up the process. The catalyst can be placed near the electrode and withdrawn when necessary, without a separation step, such as filtration, for instance.

Polarization curves

Different current density, cell and electrode potentials can be used to provide nitrate electroreduction. Therefore, polarization curves were carried out aiming to obtain values of current density and potentials that can be applied in the $NO_{3(aq)}^-$ reduction step. Current–voltage curves (CVC) were carried out in the cationic membrane, monitoring the cell (by DC power source) and electrode potential. In addition, voltammetry curves were also accomplished. All polarization and voltammetry curves were made with the nitrate concentration of 600 mg L^{-1} (135.5 N-mg L^{-1}).

Current–voltage curves (CVC)

The current–voltage curves were constructed using the DCC. At first, in order to minimize the membrane polarization phenomena, the limiting current of the cationic membrane was determined by polarization curves (Buzzi *et al.* 2013; Bittencourt *et al.* 2017). Current increments were applied using a DC power source, for 120 seconds, with a space of 180 seconds without electrical current. Then, the difference in the membrane potential was measured, as well as during the CVC construction, the cathode and the cell potential. The cathode potential was obtained using Luggin's capillary with Ag/AgCl as a reference electrode. Figure S1 (see supplementary material) shows the scheme used to obtain the values of current density and potential.

Cyclic voltammetry

A cyclic voltammetry was accomplished to investigate a specific current and potential that furthers the nitrate ion reduction. The voltammetry was made in a typical cell with three electrodes in conjunction (Autolab model PGCTAT 302N). The reference electrode was Ag/AgCl (saturated), the working electrode was copper and the counter electrode was platinum.

Electroreduction experiments

Initially Equation (3) (Plethcher 1982) was used to determine the time of reaction:

$$t = \frac{m.n.F}{I.M_w} \tag{3}$$

where 'm' is the initial concentration of nitrate in the solution (0.6 g L^{-1} of nitrate), 'F' is the Faraday constant (96,485 C mol^{-1}), 'M_w' is the nitrate molecular mass, 'I' is the current (A) and 'n' is the electron number from

the limiting step of the reaction, which in this case was value 2 (reaction of nitrate reduction to nitrite: $NO^{-}_{3(aq)} + H_2O_{(l)} + 2e^{-} \rightarrow NO^{-}_{2(aq)} + 2OH^{-}_{(aq)}$). The final value calculated was 5.2 hours, so all tests were performed for a period of 6 hours. In addition, all electroreduction assays were performed in SCC or DCC cell configurations, magnetically stirred (800 rpm–1,000 rpm) and performed at room temperature (25 °C). Tests in galvanostatic and potentiostatic modes were carried out, as well as the experiments with the application of constant cell potential. In the galvanostatic mode, the current density was fixed during the experiments and this operational mode was the most appropriate when it was not necessary to use a high process control; also, it can be easily applied on an industrial scale (Garcia-Segura *et al.* 2018). Using this mode, a study of how the different current densities can influence nitrate reduction and the products formed was conducted. Then, studies on the adjustment of pH during the experiments were done. The pH measurements and adjustments were performed using a PHTEK pH meter (model PH-3B).

In potentiostatic mode, based on the values obtained in the cyclic voltammetry, the potential of the copper electrode was fixed, with the use of a Luggin capillary with a Ag/AgCl reference electrode and with an Autolab model PGCTAT 302N potentiostat.

Experiments with a kept constant cell potential were also accomplished to evaluate the influence of this parameter.

Table 1 presents the summary of experiments carried out. After the procedures with the concentrated solution containing 600 mg L^{-1} of nitrate (135.5 N-mg L^{-1}), tests were carried out reducing the initial concentration of nitrate to 100 mg L^{-1} (22.5 N-mg L^{-1}), aiming to simulate groundwater contaminated with this ion. In these tests, Pd catalysts with different metallic charges were also used.

Calculations and analysis

Initial and final samples from the cathodic compartment were collected to determine the nitrate, nitrite and ammonium concentrations by ion chromatography (DIONEX ICS 3000 Chromatograph). The results of nitrate reduction were expressed as conversion rate X(%) (Equation 4):

$$X(\%) = \left[1 - \left(\frac{C_t}{C_o}\right)\right] \cdot 100 \quad (4)$$

where C_0 is the concentration of nitrate (N-mg L^{-1}) at the beginning of the reduction process and C_t is the concentration (N-mg L^{-1}) of nitrates at time t (6 hours).

The calculations of products formation were carried out considering the analyzed $NO^{-}_{3(aq)}$, $NO^{-}_{2(aq)}$ and $NH^{+}_{4(aq)}$ concentrations and the calculated N-gaseous compounds concentration (obtained by mass balance). The mass

Table 1 | Summary of the realized tests

Cell type	Operational mode	Parameter influence	Conditions
DCC	Cell potential fixed	Experimental potentials	7 and 9 V
DCC	Potentiostatic		–0.9 $V_{Ag/AgCl}$
DCC	Galvanostatic	Current density	0.8 mA cm^{-2} 1.2 mA cm^{-2} 1.4 mA cm^{-2}
SCC	Galvanostatic	Cell type and current density	1.2 mA cm^{-2} 1.4 mA cm^{-2}
DCC	Galvanostatic	Initial pH	2.5 4.0 6.5
DCC	Galvanostatic	pH adjustment	3–3.5 6–6.5 9–9.5
DCC	Galvanostatic	Use of catalyst, 100 mg L^{-1} and 1.4 mA cm^{-2}	Without catalyst With Pd 1.2% wt. With Pd 3.1% wt.

balance was calculated by subtracting, from the initial nitrate concentration, the nitrite, ammonium and nitrate present in the solution after 6 hours of experimental tests, considering that all other products formed are gaseous compounds and that, according to the Pourbaix diagram (Pourbaix (1963), N_2O and NO oxides formation is not likely at the experimental pH and electrodes potential, as these compounds were only intermediary products (Abdallah *et al.* 2014). Also, N_2O and NO were unstable subproducts and could be easily reduced to nitrogen (Zhang *et al.* 2019).

Catalysts characterization

To determine the composition and surface morphology of the materials used in this study, the catalysts were characterized by scanning electron microscopy (SEM) and energy dispersive spectroscopy (EDS), using a Phenom-World scanning electron microscope, equipped with an energy dispersive analytical system, operated with 15 kV of radiation.

RESULTS AND DISCUSSION

Determination of current density, and cell and electrode potentials

Current–voltage curves

In Figure 1(a), the current–voltage curves in the cationic membrane can be seen. The limiting current density value, defined by the intersection of the tangents of the first and second regions (Buzzi *et al.* 2013) was 1.57 mA cm^{-2}. The use of current densities smaller than the limiting one ($i < i_{lim}$) can minimize the concentration polarization phenomena in the membrane/solution interface (Moura *et al.* 2012). So, initially, to minimize the effect of membrane polarization, the current density applied in the electroreduction tests was 1.2 mA cm^{-2}, which corresponded to the 85% of the limiting current density value obtained in the CVC.

The cathode potential (copper electrode potential) was monitored by CVC construction (Figure 1(b)). In this experiment, inflections in 0.64 V_H and 0.75 V_H were observed. Analyzing these values for the Pourbaix diagram

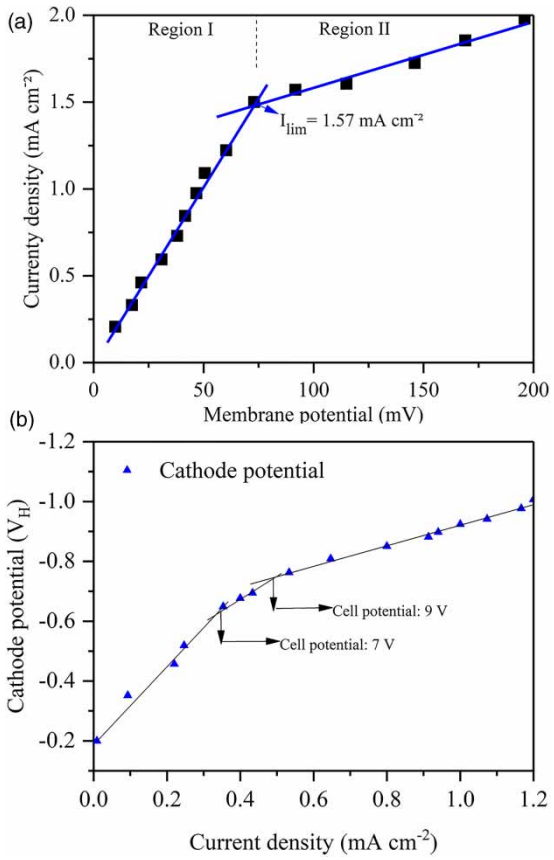

Figure 1 | (a) Membrane current–voltage curves, and (b) cathode potential curve at the initial nitrate concentration of 600 mg L^{-1} (135.5 N mg L^{-1}).

(Pourbaix 1963), and at pH 11 it was possible to observe that ammonium or nitrogen formation would be possible.

These values of cathode potential, according to the CVC obtained, correspond to 7 and 9 V in the cell potential.

The current density values obtained at these potentials were 0.4 and 0.5 mA cm^{-2}, respectively. These values of current density indicated that the membrane polarization phenomena would not occur (Bosko *et al.* 2014), since these current density values were lower than the i_{lim}. Therefore, cell potentials of 7 and 9 V were also chosen for essays with constant cell potential.

Cyclic voltammetry

The voltammetry presents a peak in the coordinate 1.4 mA cm^{-2} and -0.85 $V_{Ag/AgCl}$ (Figure S2 in supplementary material), indicating nitrate reduction to other nitrogen products. Then, electroreduction tests were also carried out in galvanostatic mode applying 1.4 mA cm^{-2} and in potentiostatic mode applying a cathode (electrode) potential of -0.9 $V_{Ag/AgCl}$.

Nitrate reduction reactions in a dual-chamber cell (DCC)

Cell potential effect

One operational way to carry out nitrate electroreduction is fixing the cell potential. To carry out these tests, the cell potential was fixed in 7 and 9 V, according to data obtained in the CVC. When a cell potential of 7 V was used, the nitrate was reduced 25 $\pm$ 3%, while with 9 V, the reduction was 37 $\pm$ 5%. When applying a cell potential of 7 V, the initial current density was 0.4 $\pm$ 0.1 mA cm^{-2} and the final was 0.58 $\pm$ 0.1 mA cm^{-2}, while at 9 V the initial value was 0.62 $\pm$ 0.1 mA cm^{-2} and the final value was 1.0 $\pm$ 0.1 mA cm^{-2}. These values of current density can explain the low nitrate reduction obtained in this variation since, probably, the hydrogen generated was not sufficient to provide the nitrate reduction, as more time was needed for the reaction to occur.

On the gaseous compound's formation (Figure 2), the formation was similar for both potentials, being higher for 9 V (10 $\pm$ 2 N-mg L^{-1}) and this probably occurs due to higher hydrogen formation in the higher current density (Zhang *et al.* 2016). The ammonium formed was lower for both variations and this also probably happens as a result of lower values of current densities reached.

Electrode potential effect: potentiostatic mode

Several electrode potentials were used with a copper electrode as described previously, for instance (Reyter *et al.* 2008) applied values of -0.9 V, -1.1 V and -1.4 V vs. Hg/HgO obtained the total relative conversion of nitrate

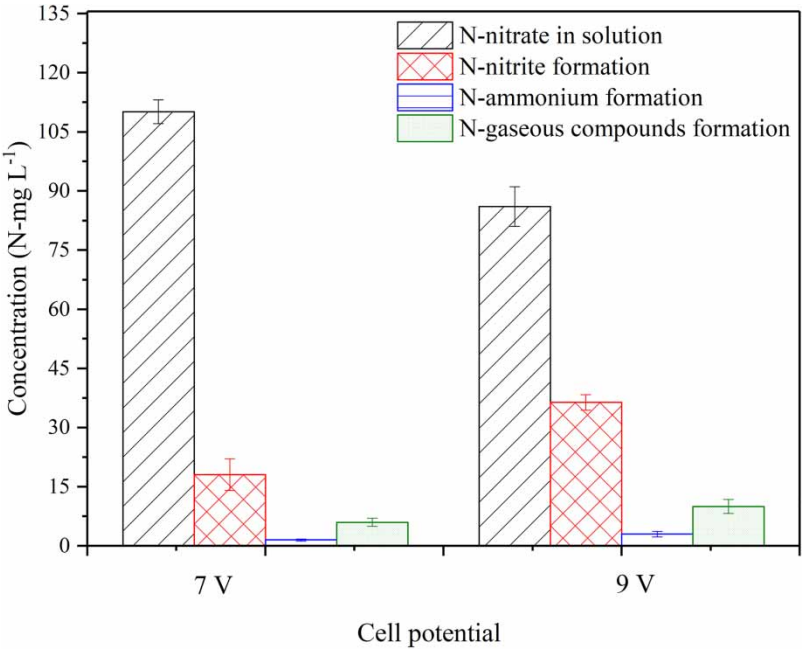

Figure 2 | Effect of constant cell potential in the nitrate reduction and compounds formed. Initial nitrate concentration: 600 mg L^{-1} (135.5 N-mg L^{-1}), 6 h of experiment.

with −1.4 V and total ammonia formation, with 250 hours of electrolysis reduction and 0.1 M $NaNO_3$ in 1 M NaOH solution (Reyter *et al.* 2008). The experiments conducted in this paper were performed applying an electrode potential of −0.9 $V_{Ag/AgCl}$ (−0.96 $V_{Hg/HgO}$), this value was determined by the cyclic voltammetry results. The results show that, at the end of the 6 hours of experiments, 20 ± 3% of the nitrate was reduced. The low value can be attributed to values of current density (Figure 3) reached in this operational parameter that decreased during the experiment. It is possible to notice that this value of reduction was similar to the one obtained when the cell potential was fixed in 7 V and the initial current density was 0.4 mA cm^{-2}.

Figure 4 shows the products formation by nitrate reduction, where practically the same values were found for the nitrite, ammonium and gaseous compounds. Studies indicated that at a potential of −1.1 E/$V_{Ag/AgCl}$ there is a predominance in the reduction of nitrate to the nitrite ion in an alkaline medium (Cattarin 1992), while at higher potentials (−1.3 $V_{Ag/AgCl}$) the main product formed is ammonia. According to Xu *et al.* (2018) the different products selectivity is related to the demands of electrons for each product formation. For instance, Kuang *et al.* (2018) tested a nitrate reduction in the range of −1.2 to −3.0 $V_{Ag/AgCl}$ (initial nitrate concentration of 50 N-mg L^{-1} with 1.0 g L^{-1} of Na_2SO_4 and Cu like electrode) and observed the highest faradaic efficiency to nitrite (44.6%) and ammonium (17.3%) when a potential of −1.2 V was applied, considering that at more negative potentials these products formations decreased.

It should be noted that the experiments performed in the potentiostatic mode are be used when greater control of the nitrate reduction is required because only the redox reactions that are thermodynamically possible in an 'E' potential occurred. However, to obtain this greater control of the process, three electrodes are required: a working electrode, a counter electrode and a reference electrode. Therefore, the galvanostatic mode, although having

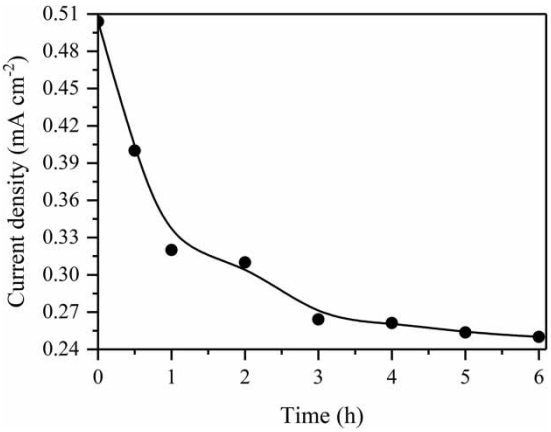

Figure 3 | Current density as a function of time. Conditions: constant cathode potential of −0.9 $V_{Ag/AgCl}$; 6 h: initial nitrate concentration of 600 mg L^{-1}.

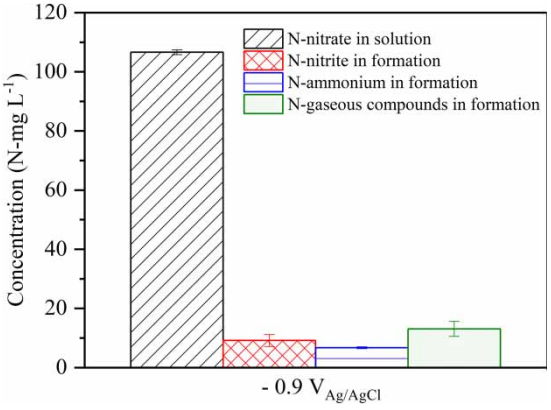

Figure 4 | Concentration of nitrogen compounds as a function of the applied cathode potential (−0.9 $V_{Ag/AgCl}$). Initial nitrate concentration: 600 mg L^{-1} (135.5 N-mg L^{-1}). 6 h of experiment.

as a characteristic a smaller control of the chemical reactions occurring during the nitrate reduction, presents applicability in industrial operations (Garcia-Segura *et al.* 2018).

After performing these experiments, it is noted that in addition to the potential of the electrode and cell, the current densities reached are an important parameter in nitrate reduction, associated with the hydrogen evolution and its role as a reducing agent. Then, tests were accomplished in galvanostatic mode setting the current density during the experiment.

Current density effect: galvanostatic mode

Several current density values were applied according to the literature, such as 0.89, 2, 5, 25, 50 and 100 mA cm^{-2} (Prasad *et al.* 2005; Kim *et al.* 2015; Zhang *et al.* 2016). However, in this study, the current density was based on the polarization curves and cyclic voltammetry. Then, tests were made with 0.8 mA cm^{-2} (current density below the limiting value found in the membrane CVC), 1.2 mA cm^{-2} and 1.4 mA cm^{-2}. It can be observed (Figure 5(a)) that the lowest nitrate reduction occurs at the lower current density (28 ± 3%, with 0.8 mA cm^{-2}). The highest nitrate reduction, 64 ± 3%, occurred at the current density of 1.4 mA cm^{-2}, while at 1.2 mA cm^{-2}, a reduction of 52 ± 2% was attained. This can be associated with the higher hydrogen content generated in higher current densities (Zhang *et al.* 2016). Figure 5(b) shows the products formations in each current density applied.

The nitrite ion was formed in all current densities studied and the ammonium formation was detected in minor quantities. The presence of nitrite in solution may be explained due to the capacity of nitrate to adsorb onto the surface of the copper electrode, then $NO_{3(aq)}^-$ is reduced to $NO_{2(aq)}^-$ (Xu *et al.* 2018; Zhang *et al.* 2021), but this ion is not efficiently reduced to gaseous compounds at the Cu surface. In addition, the presence of N-nitrite may be also related to the pH of the solution, alkaline in this experimental variation, considering that at these pH values the $NO_{2(aq)}^-$ formation is favored (Hörold *et al.* 1993). The N-ammonium formation was practically constant, between 11 and 18 N-mg L^{-1}, in all variations, however it was possible to identify greater formation at the highest applied current density. The highest current density presented an increased formation of gaseous compounds (25 ± 3 N-mg L^{-1}).

Influence of cell type

Aiming to compare the difference between nitrate reduction in a divided (DCC) and a single electroreduction cell (SCC), the $NO_{3(aq)}^-$ removal applying an electroreduction cell without membrane, in galvanostatic mode, with the current densities of 1.2 or 1.4 mA cm^2, was tested. In Table 2, it can be noticed that nitrate reduction was lower when the membrane was not used.

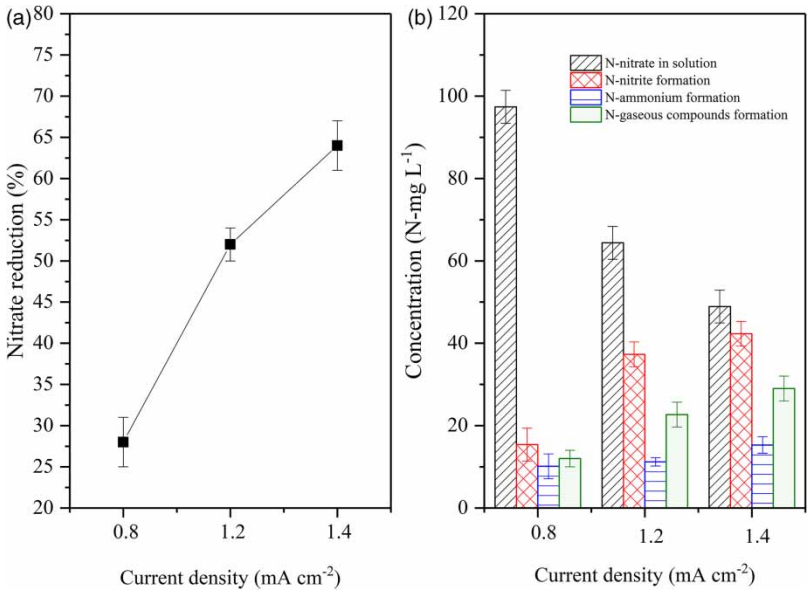

Figure 5 | Influence of current density in galvanostatic mode in the nitrate reduction with 600 mg L^{-1} of nitrate (135.5 N-mg L^{-1}). 6 h of experiment. (a) Reduction of nitrate as a function of the applied current density. (b) Concentration of nitrogen compounds as a function of applied current density.

Table 2 | Values of nitrate reduction and nitrogen compounds formation in the single chamber cell with the 600 mg L^{-1} nitrate solution (135.5 N-mg L^{-1})

Current density	Cell configuration	X (%)	Nitrite formation (N-mg L^{-1})	Ammonium formation (N-mg L^{-1})	Gaseous compounds formation (N-mg L^{-1})
1.2 mA cm^{-2}	SCC	22 ± 3%	13.9 ± 3	12.5 ± 3	3.4 ± 2
	DCC	52 ± 2%	36.6 ± 3	11.2 ± 1	22.7 ± 3
1.4 mA cm^{-2}	SCC	32 ± 3%	18.1 ± 2	13.0 ± 1	12.3 ± 4
	DCC	64 ± 3%	42.3 ± 3	15.3 ± 2	29.1 ± 3

6 h of experiment.

In a single cell, the reactions of reduction and oxidation can occur simultaneously at the cathode and anode electrode surfaces, respectively (Ding *et al.* 2015; Martínez *et al.* 2017). When the membrane was not used, the nitrate can be reduced to nitrite in the cathode electrode and reoxidized nitrate on the anode electrode (see Figure S3 in supplementary material). Therefore, the reaction is not completed to nitrogen gas. These reactions that occurred in the electrodes explain the low values of nitrate reduction. For the products, it is possible to identify a similar formation of ammonium and gaseous compounds when a current density of 1.4 mA cm^{-2} was applied. However, with both applied current densities, there was a predominance of nitrite formation, being the value formed similar to ammonium when 1.2 mA cm^{-2} was used.

pH adjustment during the experiments: galvanostatic mode in DCC

The pH value is very important in nitrogen reaction. As the better values of nitrate reduction were obtained in galvanostatic mode, different values of pH adjustment were tested during these experiments. To all variations, without pH adjustment, the final values of pH were acid in the anodic compartment (pH = 2.0) and alkaline in the cathodic one (pH = 11.5), this happening due to the reactions (Equations (5) and (6)) occurring at the electrodes (Mook *et al.* 2012):

Cathode:

$$2H^{+}_{(aq)} + 2e^{-} \rightarrow H_{2(g)} \tag{5}$$

Anode:

$$2H_2O_{(l)} \rightarrow 4H^{+}_{(aq)} + O_{2(g)} + 4e^{-} \tag{6}$$

These values of pH influence the products formations, as studies show that in an alkaline medium the main product formed is the nitrite ion (Reyter *et al.* 2008; Beltrame *et al.* 2019), in comparison to the acid media, in which the ammonium is more present in solution (Xing *et al.* 1990). Taking that into consideration, tests were made applying a current density of 1.2 mA cm^{-2}, adjusting constantly the cathodic solution's pH during the

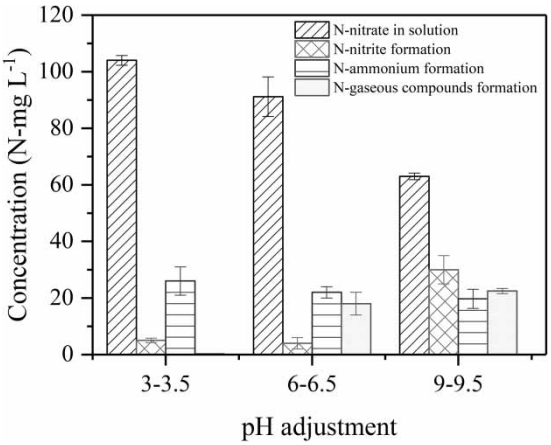

Figure 6 | Influence of pH adjusted on the nitrate reduction. Conditions: nitrate solution of 600 mg L^{-1} (135.5 N-mg L^{-1}), Current density of 1.2 mA cm^{-2}, 6 h of experiment.

experiments, adding sulfuric acid (acid pH) or sodium hydroxide (alkaline pH). The results showed that the nitrate reduction increased with increasing pH, observed as a reduction of 23 ± 2% to pH 3–3.5, a reduction of 33 ± 3% to pH 6–6.5 and a reduction of 54 ± 3% to 9–9.5 (Figure 6). The decrease in nitrate reduction at lower pH occurs due to the presence of ions in solution, such as sulphate from the added sulfuric acid (Huang *et al.* 2013), competing with the nitrate reduction and blocking the catalytic sites from copper electrodes.

The formation of gaseous compounds increased with increasing pH (Figure 6), but there was no significant difference between using pH 6–6.5 and 9–9.5. The nitrite formation was lower at acid pH and this was already reported by Garcia-Segura *et al.* (2018).

Xing *et al.* (1990) presented in their studies that under more alkaline conditions the reduction produces mainly nitrite, whereas with higher proton concentrations (H^+) a major $N_{2(g)}$ or $NH^+_{4(aq)}$ formation may happen. Under alkaline conditions, it is favorable that adsorption of oxidized materials, such as OH^- and Ox^- in the electrode and the presence of these oxides reduces the amount of available active centers of the copper electrode, which hinders the adsorption of nitrate onto the Cu surface (Martínez *et al.* 2017; Zhang *et al.* 2019).

Although the method used to regulate the pH at this work did not present itself as ideal, considering the possible adsorption of sulphate or oxidized materials in the electrode, blocking the active sites of the copper, the results showed that there was a decrease in the formation of the nitrite ion at acidic pH.

Initial pH adjustment: galvanostatic mode

The influence of the initial pH in the nitrate solution (135.5 N-mg L^{-1}) was studied using a current density of 1.4 mA cm^{-2}. The initial pH was adjusted with sulfuric acid 3 M and the current was chosen because it was obtained in the CV analysis and propitiated a good reproducibly (low standard deviation) in the experiments. Table 3 presents the results of nitrate reduction and nitrogen compounds formation using the initial pH at 2.5, 4.0 and 6.5. The nitrate reduction was 56 ± 2% to pH 2.5; 60 ± 2% to 4.0 and 64 ± 3% to 6.5, and the products formed when the initial pH was 2.5 and 4.0 were similar. In addition, the formation of the gaseous compounds was very analogous at these pH values. Therefore, it can be concluded that the initial pH, in this case, does not present a variable that can cause significant alteration in the nitrate ion reduction when the electroreduction cell operates in galvanostatic mode.

On the products side, a lot of nitrite was formed at the different initial pH and the highest gaseous compounds formation was obtained with initial pH of 6.5. Li *et al.* (2010) studied the effect of initial pH on nitrate electroreduction using an iron electrode and the authors concluded that using the initial pH of 3.0; 5.0; 7.0; 9.0 and 11.0 for electrochemical reduction of nitrate was similar for all the variations. Similar values of final reduction may be justified because of the rapid formation of hydroxyls during the nitrate reduction reactions (Equations (1) and (2)) that are occurring. This formation of OH^- favors the pH increase in all studied variations, with the main final value in the cathodic compartment being equal to 11.5.

Influence of the initial nitrate concentration and the use of Pd catalyst

Aiming to evaluate the electroreduction process to treat a MSP concentrate, tests were made with a solution with lower initial nitrate concentration (100 mg L^{-1}–22.5 N-mg L^{-1}), applying the current density of 1.4 mA cm^{-2} and without pH control (Figure 7). It was possible to notice that the nitrate reduction was higher (85 ± 4%), however the main products formed were nitrite (5.1 ± 1 N-mg L^{-1}) and ammonium (12.6 ± 2 N-mg L^{-1}) ions, with the formation of only 0.7 ± 0.3 of N-gaseous compounds. The highest formation of ammonium at this concentration occurred associated with the higher value of current density used, being that according to the study presented by Tong *et al.* (2019).

Table 3 | Influence of initial pH in the nitrate reduction with nitrate solution of 600 mg L^{-1} (135.5 N-mg L^{-1}), current density of 1.4 mA cm^{-2} at pH 2.5, pH 3.9 and pH 6.5

Initial pH	X (%)	Nitrite formation (N-mg L^{-1})	Ammonium formation (N-mg L^{-1})	Gaseous compounds formation (N-mg L^{-1})
2.5	56 ± 2%	50.8 ± 4	10.0 ± 3	15.0 ± 2
4.0	60 ± 2%	56.0 ± 2	10.1 ± 1	15.2 ± 3
6.5	64 ± 3%	42.3 ± 3	15.3 ± 2	29.1 ± 4

6 h of experiment.

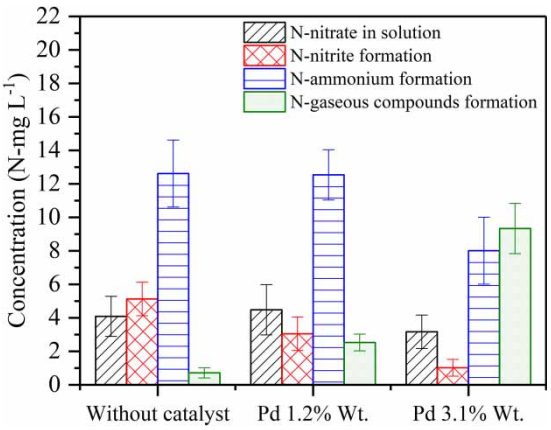

Figure 7 | Concentration of nitrogen compounds after 6 hours of operation (initial nitrate concentration 22.5 N-mg L^{-1}; 1.4 mA cm^{-2}): without catalyst, with 1.2% wt. Pd and 3.1% wt. Pd catalysts.

Comparing the values of initial nitrate concentrations applying a current density of 1.4 mA cm^{-2}, it can be inferred that with the smaller initial nitrate concentration (22.5 N-mg L^{-1}) there was a higher nitrate reduction (85 ± 4%), while with the initial nitrate concentration of 135.5 N-mg L^{-1} a reduction of 64 ± 3% was achieved. The highest nitrate reduction in the smaller initial nitrate concentration may have occurred because the electrochemical reduction is dependent on an initial adsorption in the cathode surface, since the mass transfer depends on the nitrate diffusion in the electrode by Fick's Law. At different nitrate concentrations, the active sites of the electrode can determine the occurrence or not of $NO_{3(aq)}^{-}$ reduction (da Cunha *et al.* 1996; de Groot & Koper 2004; Dima *et al.* 2005; Katsounaros & Kyriacou 2007). At this work, by using a cathodic electrode of copper with 15 cm^2, the active electrode sites can be sufficient to propitiated a major nitrate reduction on 100 mg L^{-1}.

Aiming to minimize the production of nitrite/ammonium and to improve the gaseous compounds formation (Beltrame *et al.* 2021), a catalyst impregnated with different Pd loads was tested. In the present system, copper is responsible for reducing nitrate; in turn, Pd can reduce the nitrite generated to gaseous compounds or ammonium. In this paper, the catalyst chosen was alumina in the pellets form, impregnated with Pd in the proportions of 1.2% wt. and 3.1% wt. (Figure 7).

The nitrate reduction with catalyst was practically the same without a catalyst (85 ± 4%), indicating that that the palladium does not act in the nitrate reduction (Rosca *et al.* 2009). The reduction was of 81 ± 3% when using 1.2% Pd wt. and 83 ± 3% to 3.1% Pd wt. In the presence of the catalyst, a smaller amount of nitrite was observed. The nitrite in the solution was lower when using the catalyst with Pd 3.1% wt. (1.0 ± 0.5 N-mg L^{-1}) and the ammonium formation was 8.0 ± 2 N-mg L^{-1}. The presence of the catalyst with Pd 1.2% wt. resulted in the ammonium formation being the same as the one obtained with the variance without catalyst (12.5 ± 2 N-mg L^{-1}). However, a decrease in the nitrite formation to 3.0 ± 1 N-mg L^{-1} was noted. The highest gaseous compounds formation was obtained when using a catalyst with Pd 3.1% wt., attaining a value of 9.4 ± 1.5 N-mg L^{-1}. The improvement in gaseous compounds formation can be explained due to the presence of H_{ads}, that can occur in the presence of catalysts with a high affinity to adsorb hydrogen, for example, the palladium used in these tests (Chaplin *et al.* 2012).

In general, the fact that more palladium causes a higher formation of reduction products is in line with the expectations for systems with catalytic nitrite reduction (Bosko *et al.* 2011). So, the composition, the type of support, structure of the catalyst (Martínez *et al.* 2017) and the operating parameters define which end-products are favored. The lower presence of nitrite in the solution is due to the reduction of nitrite to ammonium or nitrogen at Pd active sites (Jung *et al.* 2012; Jung *et al.* 2014; Hamid *et al.* 2018; Tokazhanov *et al.* 2020), according to the Equations 7 and 8.

$$2NO_{2(aq)}^{-} + Pd{-}4H_{ads} \rightarrow Pd^{0} + N_{2(g)} + 4OH_{(aq)}^{-} \quad (7)$$

$$NO_{2(aq)}^{-} + Pd{-}6H_{ads} \rightarrow Pd^{0} + NH_{4(aq)}^{+} + 2OH_{(aq)}^{-} \quad (8)$$

Figure S4 in supplementary material shows a scheme of the reactions that can occur at the copper electrode in the presence of palladium catalyst.

Catalysts characterization

Figure 8 shows the SEM micrographs of the materials used in this study. SEM was used to determine the morphology and disposition of the active phase. The material composition was quantified by EDS, operated in the surface mapping mode. Also, elemental composition is showed in Table 4.

In Figure 8(a), the fresh sample of Pd 1.2% catalyst shows Pd particles distributed over the entire surface of the alumina (composition determined by EDS). In Figure 8(c), Pd 3.1% wt., it can be seen that the number of particles is greater and there is also a visible population of agglomerates, compared to the Pd catalyst 1.2% wt. For the catalysts used, Figure 8(b)–8(d), it can be seen that the samples show an increase in the particle size of Pd compared to the fresh samples. This increase was more accentuated in the Pd 3.1% wt. catalyst. All Pd particles are nanometric in size. This reordering is similar to the behavior observed in reactions of catalytic elimination of nitrate in aqueous medium, using the same support and active phase (Zoppas *et al.* 2018).

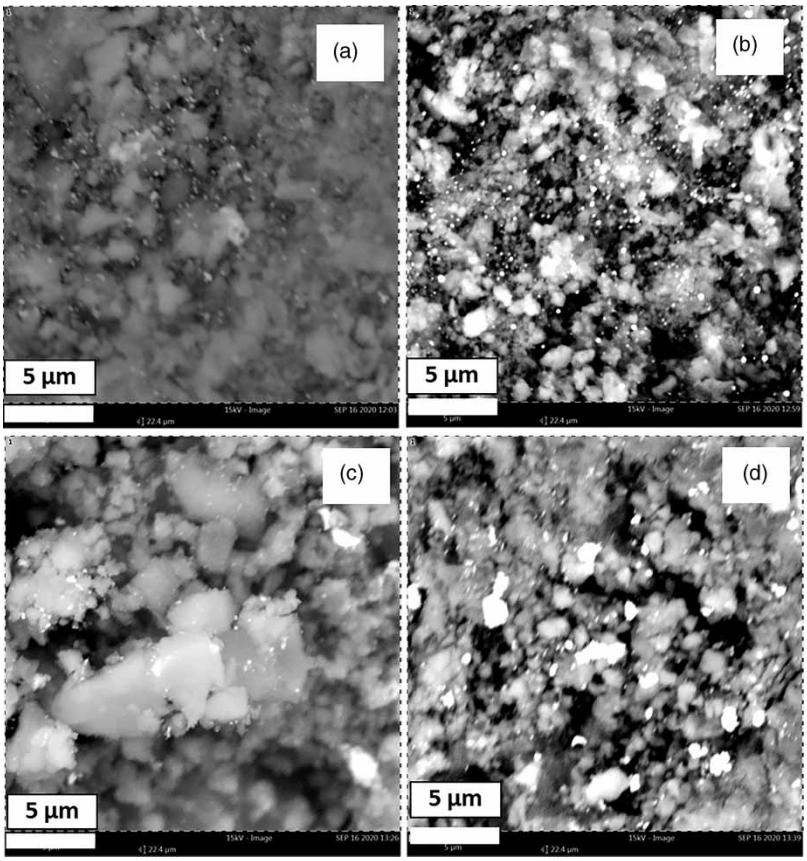

Figure 8 | Surface mapping of the catalysts supported on alumina, employed in this study. (a) Fresh Pd 1.2% wt., (b) used Pd 1.2% wt., (c) fresh Pd 3.1% wt., (d) used Pd 3.1% wt.

Table 4 | Weight concentration of the components found on the surfaces of the catalysts analyzed by SEM

	Al[a]	O[a]	Pd[a]
Fresh Pd 1.2% wt.	52.82	45.82	1.35
Used Pd 1.2% wt.	55.44	42.43	2.13
Fresh Pd 3.1% wt.	50.74	45.95	3.30
Used Pd 3.1% wt.	50.24	45.13	4.62

[a]Weight concentration.

In Table 4, the predominance of Al and O, characteristic of the support, can be seen in all samples. In addition, it was observed that the composition of the active phase for fresh samples was close to the nominal value Pd 1.2% and 3.1% wt. Furthermore, there was a superficial enrichment of the active phase, indicating that there could be a migration of Pd particles from the inside of the support to the surface.

Energy consumption

An important parameter to analyze when applying an electrochemical process is the energy consumption. Table S1 in supplementary material shows the values of energy consumption obtained in these experiments. With the DCC and 600 mg L^{-1} of nitrate, it was observed that the values of energy consumption were between 78 and 119 Kwh/N-Kg and these values were in accordance to those obtained in the Zhang *et al.* (2019) study. The highest values in the SCC (340 Kwh/N-K, 1.4 mA cm^{-2}) can be attributed to the smaller nitrate reduction compared to the one achieved with the DCC.

The highest values of energy consumption obtained at the initial nitrate concentration of 100 mg L^{-1} (524 Kwh/N-K) can occur as a response to a low nitrate concentration in the solution; also, the reduced presence of ions in the solution can cause a major resistance of the cell, causing a higher consumption of energy. The values of faradic current obtained in nitrite formation in the electroreduction with initial nitrate concentration of 135.5 N-mg L^{-1} and DCC cell are presented in the supplementary material.

CONCLUSIONS

This work shows that the electrochemical process to nitrate reduction has the potential to be used as a way of treating wastewater with high and low nitrate concentrations. With the experiments carried out it was possible to identify and to relate important parameters that can influence the electrochemical reduction of nitrate aiming at low nitrite formation. It was noticed that at alkaline pH and initial nitrate concentration of 600 mg L^{-1}, in all the current densities tested, a high nitrite concentration was formed. By applying 1.4 mA cm^{-2}, it was possible to obtain 64% nitrate reduction. At an alkaline pH, there was the highest reduction of nitrate ion compared to an acid pH, however with adjusted pH of 3–3.5 and 6–6.5 the nitrite formation was practically null.

The initial pH value was not significant for the reduction of nitrate and consequent formation of nitrogen products. The cell with two compartments presented a higher nitrate reduction than the cell with one compartment (32%, 1.4 mA cm^{-2}). For the nitrate concentration of 100 mg L^{-1}, with and without Pd catalyst, the nitrate reduction was similar (82%); but considering the products formation, with a catalyst of 3.1% wt. Pd, the nitrite formation was only 1.0 N-mg L^{-1} and the gaseous compound formation was 9.4 N-mg L^{-1}. In this study, the catalyst was placed close to the copper electrode, and not added to the nitrate solution. Therefore, there was no need for a further filtration step to separate the catalyst from the solution, yielding a novel electrocatalytic system.

Lastly, it was possible to notice that operational parameters like current density, type of cell, pH, initial nitrate concentration and catalyst can influence electrochemical nitrate reduction and, consequently, the products formed, therefore it will be necessary to carry out more studies and tests on this topic.

ACKNOWLEDGEMENTS

The financial support of the Brazilian funding agencies Conselho Nacional de Desenvolvimento Científico e Tecnológico – CNPq/Brazil, Fundação de Amparo à Pesquisa do Estado do Rio Grande do Sul FAPERGS/Brazil, Financiadora de Estudos e Projetos -FINEP/Brazil and from the Ibero-American Program on Science and Technology for Development (CYTED) are acknowledged. The authors would like to thank Régis Araujo for the English review.

DATA AVAILABILITY STATEMENT

All relevant data are included in the paper or its Supplementary Information.

REFERENCES

Abdallah, R., Geneste, F., Labasque, T., Djelal, H., Fourcade, F., Amrane, A., Taha, S. & Floner, D. 2014 Selective and quantitative nitrate electroreduction to ammonium using a porous copper electrode in an electrochemical flow cell. *Journal of Electroanalytical Chemistry* **727**, 148–153. https://doi.org/10.1016/j.jelechem.2014.06.016.

Beltrame, T. F., Coelho, V., Marder, L., Ferreira, J. Z., Marchesini, F. A. & Bernardes, A. M. 2018 Effect of operational parameters and Pd/In catalyst in the reduction of nitrate using copper electrode. *Environmental Technology* **39** (22), 2835–2847. https://doi.org/10.1080/09593330.2017.1367422.

Beltrame, T. F., Zoppas, F. M., Marder, L., Marchesini, F. A., Miró, E. & Bernardes, A. M. 2019 Use of a two-step process to denitrification of synthetic brines: electroreduction in a dual-chamber cell and catalytic reduction. *Environmental Science and Pollution Research*. https://doi.org/10.1007/s11356-019-06763-x.

Beltrame, T. F., Gomes, M. C., Marder, L., Marchenisi, F. A., Ulla, M. A. & Bernardes, A. M. 2020 Use of copper plate electrode and Pd catalyst to the nitrate reduction in an electrochemical dual-chamber cell. *Journal of Water Process Engineering* **35**, 101189. https://doi.org/doi.org/10.1016/j.jwpe.2020.101189.

Beltrame, T. F., Zoppas, F. M., Gomes, M. C., Ferreira, J. Z., Marchesini, F. A. & Bernardes, A. M. 2021 Electrochemical nitrate reduction of brines: improving selectivity to N_2 by the use of Pd/activated carbon fiber catalyst. *Chemosphere* 130832. https://doi.org/10.1016/j.chemosphere.2021.130832.

Bittencourt, S. D., Marder, L., Benvenuti, T., Ferreira, J. Z. & Bernardes, A. M. 2017 Analysis of different current density conditions in the electrodialysis of zinc electroplating process solution. *Separation Science and Technology* **52** (13), 2079–2089. https://doi.org/10.1080/01496395.2017.1310896.

Bosko, M. L., Marchesini, F. A., Cornaglia, L. M. & Miró, E. E. 2011 Controlled Pd deposition on carbon fibers by electroless plating for the reduction of nitrite in water. *Catalysis Communications* **16** (1), 189–193. https://doi.org/10.1016/j.catcom.2011.09.034.

Bosko, M. L., Rodrigues, M. A. S., Ferreira, J. Z., Miró, E. E. & Bernardes, A. M. 2014 Nitrate reduction of brines from water desalination plants by membrane electrolysis. *Journal of Membrane Science* **451**, 276–284. https://doi.org/10.1016/j.memsci.2013.10.004.

Buzzi, D. C., Viegas, L. S., Rodrigues, M. A. S., Bernardes, A. M. & Tenório, J. A. S. 2013 Water recovery from acid mine drainage by electrodialysis. *Minerals Engineering* **40**, 82–89. https://doi.org/10.1016/j.mineng.2012.08.005.

Cameron, K. C., Di, H. J. & Moir, J. L. 2013 Nitrogen losses from the soil/plant system: a review: nitrogen losses. *Annals of Applied Biology* **162** (2), 145–173. https://doi.org/10.1111/aab.12014.

Cattarin, S. 1992 Electrochemical reduction of nitrogen oxyanions in 1 M sodium hydroxide solutions at silver, copper and cuinse$_2$ electrodes. *Journal of Applied Electrochemistry* **22** (11), 1077–1081. https://doi.org/10.1007/BF01029588.

Chaplin, B. P., Reinhard, M., Schneider, W. F., Schüth, C., Shapley, J. R., Strathmann, T. J. & Werth, C. J. 2012 Critical review of Pd-based catalytic treatment of priority contaminants in water. *Environmental Science & Technology* **46** (7), 3655–3670. https://doi.org/10.1021/es204087q.

da Cunha, M. C. P. M., Weber, M. & Nart, F. C. 1996 On the adsorption and reduction of NO_3^- ions at Au and Pt electrodes studied by in situ FTIR spectroscopy. *Journal of Electroanalytical Chemistry* **414**, 163–170.

de Groot, M. T. & Koper, M. T. M. 2004 The influence of nitrate concentration and acidity on the electrocatalytic reduction of nitrate on platinum. *Journal of Electroanalytical Chemistry* **562** (1), 81–94. https://doi.org/10.1016/j.jelechem.2003.08.011.

Dima, G. E., Beltramo, G. L. & Koper, M. T. M. 2005 Nitrate reduction on single-crystal platinum electrodes. *Electrochimica Acta* **50** (21), 4318–4326. https://doi.org/10.1016/j.electacta.2005.02.093.

Ding, J., Li, W., Zhao, Q.-L., Wang, K., Zheng, Z. & Gao, Y.-Z. 2015 Electroreduction of nitrate in water: role of cathode and cell configuration. *Chemical Engineering Journal* **271**, 252–259. https://doi.org/10.1016/j.cej.2015.03.001.

Dortsiou, M., Katsounaros, I., Polatides, C. & Kyriacou, G. 2013 Influence of the electrode and the pH on the rate and the product distribution of the electrochemical removal of nitrate. *Environmental Technology* **34** (3), 373–381. https://doi.org/10.1080/09593330.2012.696722.

Estudillo-Wong, L. A., Arce-Estrada, E. M., Alonso-Vante, N. & Manzo-Robledo, A. 2011 Electro-reduction of nitrate species on Pt-based nanoparticles: surface area effects. *Catalysis Today* **166** (1), 201–204. https://doi.org/10.1016/j.cattod.2010.09.010.

Garcia-Segura, S., Lanzarini-Lopes, M., Hristovski, K. & Westerhoff, P. 2018 Electrocatalytic reduction of nitrate: fundamentals to full-scale water treatment applications. *Applied Catalysis B: Environmental* **236**, 546–568. https://doi.org/10.1016/j.apcatb.2018.05.041.

Gwak, J., Ahn, S., Baik, M.-H. & Lee, Y. 2019 One metal is enough: a nickel complex reduces nitrate anions to nitrogen gas. *Chemical Science* **10** (18), 4767–4774. https://doi.org/10.1039/C9SC00717B.

Hamid, S., Bae, S. & Lee, W. 2018 Novel bimetallic catalyst supported by red mud for enhanced nitrate reduction. *Chemical Engineering Journal* **348**, 877–887. https://doi.org/10.1016/j.cej.2018.05.016.

Hörold, S., Vorlop, K.-D., Tacke, T. & Sell, M. 1993 Development of catalysts for a selective nitrate and nitrite removal from drinking water. *Catalysis Today* **17** (1–2), 21–30.

Huang, H., Zhao, M., Xing, X., Bae, I. T. & Scherson, D. 1990 *In-situ* infrared studies of the Cd-UPD mediated reduction of nitrate on gold. *Journal of Electroanalytical Chemistry and Interfacial Electrochemistry* **293** (1–2), 279–284. https://doi.org/10.1016/0022-0728(90)80071-D.

Huang, W., Li, M., Zhang, B., Feng, C., Lei, X. & Xu, B. 2013 Influence of operating conditions on electrochemical reduction of nitrate in groundwater. *Water Environment Research* **85** (3), 224–231. https://doi.org/10.2175/106143012X13418552642047.

Jonoush, Z. A., Rezaee, A. & Ghaffarinejad, A. 2020 Electrocatalytic nitrate reduction using Fe0/Fe_3O_4 nanoparticles immobilized on nickel foam: selectivity and energy consumption studies. *Journal of Cleaner Production* **242**, 118569. https://doi.org/10.1016/j.jclepro.2019.118569.

Jung, J., Bae, S. & Lee, W. 2012 Nitrate reduction by maghemite supported Cu-Pd bimetallic catalyst. *Applied Catalysis B: Environmental* **127**, 148–158. https://doi.org/10.1016/j.apcatb.2012.08.017.

Jung, S., Bae, S. & Lee, W. 2014 Development of Pd–Cu/hematite catalyst for selective nitrate reduction. *Environmental Science & Technology* **48** (16), 9651–9658. https://doi.org/10.1021/es502263p.

Katsounaros, I. & Kyriacou, G. 2007 Influence of the concentration and the nature of the supporting electrolyte on the electrochemical reduction of nitrate on tin cathode. *Electrochimica Acta* **52** (23), 6412–6420. https://doi.org/10.1016/j.electacta.2007.04.050.

Khomutov, N. E. & Stamkulov, U. S. 1971 Nitrate reduction at various metal electrodes. *Soviet Electrochemistry* **7**, 312–316.

Kim, Y. J., Lee, K., Cha, H. Y., Yoo, K. M., Jeon, C. S., Kim, H. J., Kim, D. & Park, K. Y. 2015 Electrolytic denitrification with an ion-exchange membrane in groundwater. *Water Science and Technology: Water Supply* **15** (6), 1320–1325. https://doi.org/10.2166/ws.2015.079.

Kuang, P., Natsui, K. & Einaga, Y. 2018 Comparison of performance between boron-doped diamond and copper electrodes for selective nitrogen gas formation by the electrochemical reduction of nitrate. *Chemosphere* **210**, 524–530. https://doi.org/10.1016/j.chemosphere.2018.07.039.

Li, M., Feng, C., Zhang, Z., Yang, S. & Sugiura, N. 2010 Treatment of nitrate contaminated water using an electrochemical method. *Bioresource Technology* **101** (16), 6553–6557. https://doi.org/10.1016/j.biortech.2010.03.076.

Martínez, J., Ortiz, A. & Ortiz, I. 2017 State-of-the-art and perspectives of the catalytic and electrocatalytic reduction of aqueous nitrates. *Applied Catalysis B: Environmental* **207**, 42–59. https://doi.org/10.1016/j.apcatb.2017.02.016.

Mook, W. T., Chakrabarti, M. H., Aroua, M. K., Khan, G. M. A., Ali, B. S., Islam, M. S. & Abu Hassan, M. A. 2012 Removal of total ammonia nitrogen (TAN), nitrate and total organic carbon (TOC) from aquaculture wastewater using electrochemical technology: a review. *Desalination* **285**, 1–13. https://doi.org/10.1016/j.desal.2011.09.029.

Moura, R. C. A., Bertuol, D. A., Ferreira, C. A. & Amado, F. D. R. 2012 Study of chromium removal by the electrodialysis of tannery and metal-finishing effluents. *International Journal of Chemical Engineering* **2012**, 1–7. https://doi.org/10.1155/2012/179312.

Pérez-Gallent, E., Figueiredo, M. C., Katsounaros, I. & Koper, M. T. M. 2017 Electrocatalytic reduction of Nitrate on Copper single crystals in acidic and alkaline solutions. **227** (10), 77–84. https://doi.org/10.1016/j.electacta.2016.12.147.

Plethcher, D. 1982 *Industrial Electrochemistry*. New York: Chapman and Hall Ltd.

Pourbaix, M. 1963 *Atlas D'equilibres Electrochimiques*. Paris: Gauthier-Villars.

Prasad, P. K. R., Priya, M. N. & Palanivelu, K. 2005 Nitrate removal from groundwater using electrolytic reduction method. *Indian Journal of Chemical Technology* **12**, 164–169.

Reyter, D., Bélanger, D. & Roué, L. 2008 Study of the electroreduction of nitrate on copper in alkaline solution. *Electrochimica Acta* **53** (20), 5977–5984. https://doi.org/10.1016/j.electacta.2008.03.048.

Rosca, V., Duca, M., de Groot, M. T. & Koper, M. T. M. 2009 Nitrogen cycle electrocatalysis. *Chemical Reviews* **109** (6), 2209–2244. https://doi.org/10.1021/cr8003696.

Sahli, M. A. M., Annouar, S., Mountadar, M., Soufiane, A. & Elmidaoui, A. 2008 Nitrate removal of brackish underground water by chemical adsorption and by electrodialysis. *Desalination* **227**, 327–333.

Simpson, B. K. & Johnson, D. C. 2004 Electrocatalysis of nitrate reduction at copper-nickel alloy electrodes in acidic media. *Electroanalysis* **16** (7), 532–538. https://doi.org/10.1002/elan.200302790.

Smith, V. H. & Schindler, D. W. 2009 Eutrophication science: where do we go from here? *Trends in Ecology & Evolution* **24** (4), 201–207. https://doi.org/10.1016/j.tree.2008.11.009.

Su, J. F., Ruzybayev, I., Shah, I. & Huang, C. P. 2016 The electrochemical reduction of nitrate over micro-architectured metal electrodes with stainless steel scaffold. *Applied Catalysis B: Environmental* **180**, 199–209. https://doi.org/10.1016/j.apcatb.2015.06.028.

Tokazhanov, G., Ramazanova, E., Hamid, S., Bae, S. & Lee, W. 2020 Advances in the catalytic reduction of nitrate by metallic catalysts for high efficiency and N_2 selectivity: a review. *Chemical Engineering Journal* **384**, 123252. https://doi.org/10.1016/j.cej.2019.123252.

Tong, S., Liu, H., Feng, C., Chen, N., Zhao, Y., Xu, B., Zhao, J. & Zhu, M. 2019 Stimulation impact of electric currents on heterotrophic denitrifying microbial viability and denitrification performance in high concentration nitrate-contaminated wastewater. *Journal of Environmental Sciences* **77**, 363–371. https://doi.org/10.1016/j.jes.2018.09.014.

Wang, Y., Wang, C., Li, M., Yu, Y. & Zhang, B. 2021 Nitrate electroreduction: mechanism insight, in situ characterization, performance evaluation, and challenges. *Chemical Society Reviews*. https://: 10.1039/D1CS00116G.

Xing, X., Scherson, D. A. & Mak, C. 1990 The electrocatalytic reduction of nitrate mediated by underpotentiaI-deposited cadmium on gold and silver electrodes in acid media. *Journal of the Electrchemical Society* **137** (7), 2166–2175.

Xu, D., Li, Y., Yin, L., Ji, Y., Niu, J. & Yu, Y. 2018 Electrochemical removal of nitrate in industrial wastewater. *Frontiers of Environmental Science & Engineering* **12** (1). https://doi.org/10.1007/s11783-018-1033-z.

Ye, W., Zhang, W., Hu, X., Yang, S. & Liang, W. 2020 Efficient electrochemical-catalytic reduction of nitrate using Co/AC0.9-AB0.1 particle electrode. *Science of the Total Environment* **732**, 139245. https://doi.org/10.1016/j.scitotenv.2020.139245.

Zhang, Q., Ding, L., Cui, H., Zhai, J., Wei, Z. & Li, Q. 2014 Electrodeposition of Cu-Pd alloys onto electrophoretic deposited carbon nanotubes for nitrate electroreduction. *Applied Surface Science* **308**, 113–120. https://doi.org/10.1016/j.apsusc.2014.04.119.

Zhang, Z., Xu, Y., Shi, W., Wang, W., Zhang, R., Bao, X., Zhang, B., Li, L. & Cui, F. 2016 Electrochemical-catalytic reduction of nitrate over Pd–Cu/γAl_2O_3 catalyst in cathode chamber: enhanced removal efficiency and N_2 selectivity. *Chemical Engineering Journal* **290**, 201–208. https://doi.org/10.1016/j.cej.2016.01.063.

Zhang, L., Yin, D., Zhai, S., Liu, Y., Dou, C., Chen, P. & Huang, G. 2019 Electrochemical behaviors and influence factors of copper and copper alloys cathode for electrocatalytic nitrate removal. *Water Environment Research* **91** (12), 1589–1599. https://doi.org/10.1002/wer.1151.

Zhang, X., Wang, Y., Liu, C., Yu, Y., Lu, S. & Zhang, B. 2021 Recent advances in non-noble metal electrocatalysts for nitrate reduction. *Chemical Engineering Journal* **403**, 126269. https://doi.org/10.1016/j.cej.2020.126269.

Zoppas, F. M., Bernardes, A., Miró, E. E. & Marchesini, F. A. 2018 Nitrate reduction of brines from water desalination plants employing a low metallic charge Pd, in catalyst and formic acid as reducing agent. *Catalysis Letters* **148** (8), 2572–2584. https://doi.org/10.1007/s10562-018-2429-x.

First received 12 April 2021; accepted in revised form 25 May 2021. Available online 4 June 2021